

Fourier Harmonics of High- p_T Particles Probing the Fluctuating Initial Condition Geometries in Heavy-Ion Collisions

Barbara Betz,¹ Miklos Gyulassy,¹ and Giorgio Torrieri^{1,2}

¹*Department of Physics, Columbia University, New York, 10027, USA*

²*Frankfurt Institute for Advanced Studies (FIAS), Frankfurt am Main, Germany*

While the 2nd Fourier harmonics of jet quenching have been thoroughly explored in the literature and shown to be sensitive to the underlying jet path-length dependence of energy loss and the differences between the mean eccentricity predicted by Glauber and CGC/KLN models of initial conditions, the sensitivity of higher harmonics has remained relatively unexplored. We demonstrate that those higher-jet harmonics are remarkably insensitive to the initial conditions, stress the impact of including an energy dependence in the energy-loss prescription, and show that higher powers of the path-length dependence will lead to a saturation effect for all Fourier harmonics. However, the different $v_n(N_{part})$ vs. $v_n^{AA}(N_{part})$ correlations between the moments of monojet and dijet nuclear modifications factors remain the most sensitive probe to differentiate between Glauber and CGC/KLN initial state sQGP geometries.

PACS numbers: 12.38.Mh,13.87.24.85.+p

I. INTRODUCTION

Heavy-ion collisions at the Relativistic Heavy Ion Collider (RHIC) indicate the production of an opaque (i.e. strongly jet-suppressing) [1–5], strongly-coupled, fast-thermalizing medium that possibly needs to be described using methods derived from AdS/CFT string theory [6]. However, so far neither the initial conditions of the collisions nor the microscopic dynamics of the jet-energy loss are conclusively understood.

Two models are commonly used to characterize the initial conditions. The Glauber model [7], describing incoherent superpositions of proton-proton collisions, and the “Color Glass Condensate” (CGC) [8], given e.g. by the KLN model [9, 10], where saturation effects are taken into account. They differ by their initial temperature gradients, their initial high- p_T parton distribution, and the distance travelled by each parton, leading to a different opacity estimate and show large event-by-event fluctuations [11–15].

The jet-energy loss can either be described as multiple scatterings of the parton [16–21], specific for a weakly-coupled pQCD medium, or using the AdS/CFT correspondence where the problem of a parton stopped in a thermal medium is related to the problem of a string falling into a 5-dimensional black hole [22–25].

Experimentally, jet-energy loss is parametrized by the suppression factor R_{AA} , defined as the ratio of jets produced in $A+A$ collisions to the expectation for jets being produced in $p+p$ collisions

$$R_{AA}(p_T) = \frac{dN^{A+A}/dp_T}{N_{coll}dN^{p+p}/dp_T}, \quad (1)$$

where N_{coll} is the number of collisions, a theoretical parameter (calculated within the Glauber model [13]) depending on centrality (i.e., on the number of participants N_{part}).

The first attempt to disentangle the initial conditions

while simultaneously describing the nuclear modification factor $R_{AA}(N_{part})$ and the elliptic flow $v_2(N_{part})$ was given in Refs. [26, 27], favoring a strongly-coupled energy loss. To further study the differences of a pQCD and AdS/CFT-like energy loss, we investigate the role of the energy dependence in the energy-loss prescription, examine the power of the path-length dependence, and calculate higher-jet harmonics.

In the high-temperature limit, all dependences on the intrinsic scales of the system (T_c, Λ_{QCD} , etc.) disappear. Because of this, a generic energy-loss rate dE/dx is given by an arbitrary combination of dimensionful parameters constrained by the total dimension of the observable and the requirement that faster particles and hotter media result in a bigger suppression. We choose

$$\frac{dE}{dx}(\vec{x}_0, \phi, \tau) = -\kappa P^a \tau^z T^{z-a+2} [\vec{x}_0 + \hat{n}(\phi)\tau, \tau], \quad (2)$$

where P is the momentum of the jet(s) considered and a, z are parameters controlling the jet energy (momentum) and path-length dependence, respectively. In the Bethe-Heitler limit $a = 1$ and $z = 0$, while in the deep LPM pQCD limit $a \sim 0$ and $z \sim 1$. If $a = 0$ and $z = 2$, our model coincides with the model referred to as “AdS/CFT” in Refs. [26, 27]. However, on-shell AdS/CFT calculations [22–25] show that $a = 1/3$ and $z = 2$, thus we are going to consider $a = 1/3$ throughout the whole paper. We note that, as it is clearly shown in Refs. [22–25], $z = 2$ is only a *lower* limit corresponding to an “on-shell” quark whose stopping distance is $l_f \gg 1/T$ and whose initial energy is $E_0 \gg T$. In a realistic medium, the first assumption is likely to be violated, resulting in values possibly of $z > 2$.

In a static medium, $dE/dx \sim \tau^z$, while in a dynamic medium, dE/dx will acquire additional powers of τ due to the dependence of temperature on τ , implicitly included in Eq. (2). Here, we assume a 1D Bjorken expansion [28]

$$T(\vec{x}, \tau) = T_0(\vec{x}) \left(\frac{T_0}{\tau} \right)^{1/3}, \quad (3)$$

and $\tau_0 = 1fm$, in line with Ref. [29].

In a particular case of radiative-dominated scattering in the LPM regime, $\kappa T^3 \sim \hat{q}$ [30]. In general, κ measures the interaction cross-section, while T^3 is related to the density of scattering centers. This (like soft observables in general) can be used as a constraint for κ , but additionally one has to assume nearly complete thermalization on the timescale of jet propagation throughout the system as well as a straight-forward relation between entropy density and multiplicity. While these assumptions are reasonable, they are not easily falsifiable, and, in particular, in the \hat{q} -limit, one finds that κ can *not* describe jet quenching and a realistic gluon density at the same time [30]. Therefore, we limit ourselves to fitting κ to R_{AA} , disregarding any interpretation in terms of the density of soft degrees of freedom, comparing to the data on (ϕ, \vec{x}_0) -averaged R_{AA} versus centrality for a range of $E_f \sim 6 - 9$ GeV [31].

Considering that R_{AA} is given by the ratio of jets in the QGP to jets in vacuum, one obtains the following formula for the nuclear modification factor from Eq. (2)

$$R_{AA}(\vec{x}_0, \phi, N_{part}) = \exp[-\chi(\vec{x}_0, \phi, P_f)], \quad (4)$$

with

$$\chi(\vec{x}_0, \phi, P_f) = \left(\frac{1+a-n}{1-a} \right) \ln \left[1 - \frac{K}{P_0^{1-a}} I(a, z, \phi, \vec{x}_0) \right], \quad (5)$$

and

$$I(a, z, \phi, \vec{x}_0) = \int_{\tau_0}^{\infty} \tau^z T^{z-a+2} [\vec{x}_0 + \hat{n}(\phi)\tau, \tau] d\tau. \quad (6)$$

n is the spectral index (taken to be $n \sim 6$), and $K = \kappa(1-a)$.

In case of $a = 1$ (the Bethe-Heitler limit), $1/(1-a)$ diverges, but since $K = \kappa(1-a) \rightarrow 0$,

$$\chi(\vec{x}_0, \phi, P_f, a = 1) = \kappa(n-2)I(a, z, \phi, \vec{x}_0). \quad (7)$$

From the above calculated $R_{AA}(\vec{x}_0, \phi, N_{part})$, the $R_{AA}(N_{part})$ can be obtained by averaging over all possible \vec{x}_0 and ϕ

$$R_{AA}(N_{part}) = \frac{\int R_{AA}(\vec{x}_0, \phi) T_{AA}(\vec{x}_0) d\vec{x}_0 d\phi / (2\pi)}{\int T_{AA}(\vec{x}_0) d\vec{x}_0}, \quad (8)$$

where the nuclear overlap function is used in case of the Glauber model and $T_{AA} = \rho^2/P_0^2$ for the CGC prescription.

After having fixed κ , the v_n can be computed via

$$v_n(N_{part}) = \frac{\int d\phi \cos\{n[\phi - \psi_n]\} R_{AA}(\phi)}{\int d\phi R_{AA}(\phi)}. \quad (9)$$

The Fourier density components e_n and the reaction-plane axis ψ_n are determined according to the initial density distribution used in Ref. [15]

$$e_n(t) = \frac{\sqrt{\langle r^2 \cos(n\phi) \rangle^2 + \langle r^2 \sin(n\phi) \rangle^2}}{\langle r^2 \rangle} \quad (10)$$

and

$$\psi_n(t) = \frac{1}{n} \tan^{-1} \frac{\langle r \sin(n\phi) \rangle}{\langle r \cos(n\phi) \rangle}. \quad (11)$$

Here, $\theta = \tan^{-1}(x/y)$ is the angle w.r.t. which the reaction plane eccentricity is defined. By definition, the impact parameter points into the x -direction, but event-by-event fluctuations introduce non-trivial and harmonic dependent ψ_n 's.

We checked that we reproduce the results of Ref. [26] when our approach is simplified to the one used in this reference, where

$$R_{AA}(N_{part}) = \langle e^{-\kappa I_m} \rangle, \quad (12)$$

and

$$I_m = \int_0^\infty dl l^{m-1} \rho(\vec{r} + l\hat{v}), m = 1, 2, \dots \quad (13)$$

However, one of the main differences to our approach is that we also consider the energy dependence in the jet-energy loss. In other words, $a = 0$ in Refs. [26, 27] while we assume $a = 0.3$ [see Eq. (2)] throughout the whole study.

The above analysis can be extended to dijets, analogously to Ref. [27]. Dijet suppression is parametrized by the factor I_{AA} , the ratio of the dijet suppression to the suppression of jets. Experimentally, I_{AA} is defined as [32]

$$I_{AA} = \frac{dN_{dijet}^{A+A}/dp_T}{R_{AA} dN_{dijet}^{P+P}/dp_T}. \quad (14)$$

Clearly, a higher I_{AA} than R_{AA} , as observed in Ref. [32] implies that if one jet survives, the other one has a higher probability to survive as well. In turn, this indicates that jets emitted from less dense periphery regions have a larger impact. Thus, as remarked in Ref. [32], comparing jet abundance to dijet abundance can be a sensitive medium probe.

II. RESULTS AND DISCUSSION

A. Mean Correlations

We have carried out the procedure described in the previous section for a variety of impact parameters and initial conditions. In this subsection, we focus on the mean correlations. The width of these correlations and will be discussed in the following subsection. Please note that this width is the actual physical geometry fluctuation.

Throughout the paper, we distinguish four different cases. The Glauber model [7] and the CGC/KLN prescription [8–10], both event-by-event and averaged over many events, i.e. in the latter case the initial conditions are smoothed over many events and the energy loss is calculated subsequently.

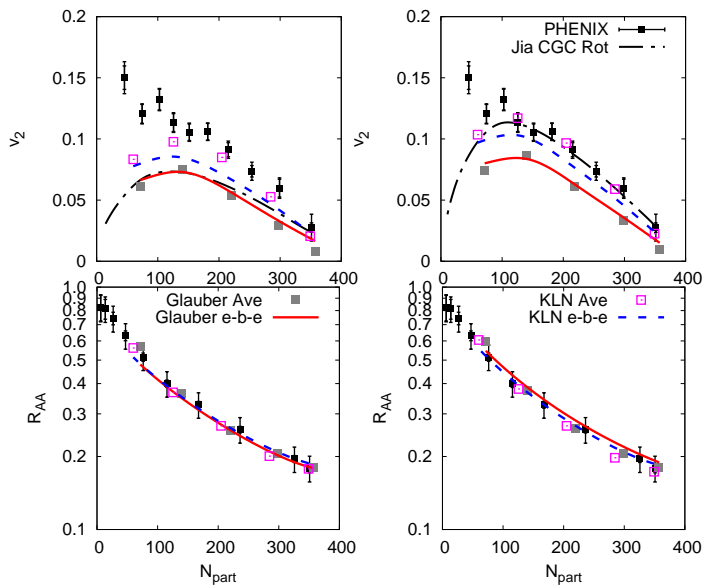


FIG. 1: v_2 (top panels) and R_{AA} (bottom panels) of high-momentum particles as a function of the number of participants, N_{part} , for $z = 1$ (left panel) and $z = 2$ [right panel, see Eq. (2) for definition]. The data are taken from Ref. [31].

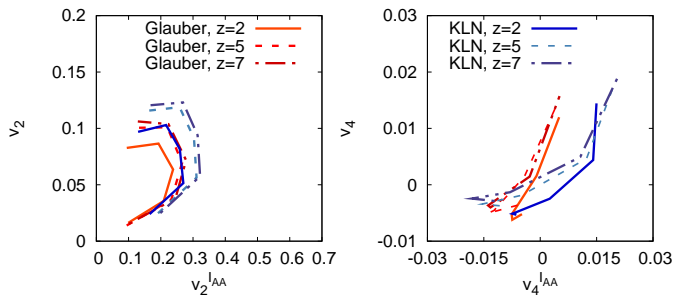


FIG. 2: Higher Fourier coefficients of dijet observables, v_2^{IAA} vs. v_2 (left panel) and v_4^{IAA} vs. v_4 (right panel) for the Glauber model (reddish lines) and the KLN model (greyish lines) for $z = 2, 5, 7$. A clear shift between the Glauber and the KLN model as well as a saturation effect for larger z can be seen.

Fig. 1 shows that for all initial conditions and parameters in the jet-energy loss formalism chosen the $R_{AA}(N_{part})$ can be fitted by an appropriate value for κ . In contrast to Ref. [27] this κ is the same for both parts of the dijet. When calculating I_{AA} , our results meet the datapoint of Ref. [33] for both Glauber and CGC/KLN initial conditions.

Moreover, the figure reveals that once the $R_{AA}(N_{part})$ is fixed, small differences occur in $v_2(N_{part})$ for the two initial conditions considered. The difference to the fit by Jia et al. [26] (black long dashed-dotted line) is due to the additional energy loss dependence, parametrized by $a = 0.3$. Interestingly enough, in contrast to the Glauber events, the averaged CGC events show a larger $v_2(N_{part})$ than the event-by-event analysis.

However, Fig. 1 basically confirms the results of Ref. [26]. Having fixed the $R_{AA}(N_{part})$, the $v_2(N_{part})$ can be reproduced well by choosing KLN initial conditions and a jet energy length scale with $z \geq 2$.

Since the energy loss calculated by AdS/CFT [22–25] clearly states that $z = 2$ is only a lower limit, this raises the question which power in the jet path-length dependence has to be considered. A detailed discussion of this issue will follow in the next subsection (see the Fig. 7).

Before that, we will focus on correlations of higher Fourier coefficients of dijet observables, v_2^{IAA} vs. v_2 and v_4^{IAA} vs. v_4 . Fig. 2 displays those correlations for the Glauber (reddish lines) and the KLN model (greyish lines) for $z = 2, 5, 7$.

A clear saturation effect occurs for larger z as well as a shift between the Glauber and the KLN model. Please note that while for the v_2 correlation larger values of z of the Glauber model coincide with lower values of the KLN model, this is no longer true for the v_4 correlations. Therefore, the different means of the correlations between $v_n(p_T)$ vs. $v_n^{IAA}(p_T)$ remain the most sensitive probe to differentiate between CGC and Glauber initial state geometries.

B. The Shallowness of the Correlations

After having focussed on the mean correlations in the last subsection, we now want to investigate the width of these correlations which is extremely important to conclude about the significance of the previously shown differences in the path-length dependence of the energy loss and the initial states considered.

Figs. 3 and 4 are a repetition of Figs. 1 and 2, including the fluctuations for the event-by-event analysis. As can be seen, those fluctuations are small for $R_{AA}(N_{part})$, but the width for the $v_2(N_{part})$ is rather large. Thus, in an experimental analysis it is less straightforward to distinguish between the different initial conditions than originally hoped for. The same is true for the coefficients of dijet observables in Fig. 4. Here it becomes obvious that the while larger Fourier coefficients become smaller, their width becomes larger. Therefore, it is necessary to always determine the mean and the width of the correlations considered.

While the 2nd Fourier harmonics of jet quenching have been thoroughly investigated [26, 27, 34], the sensitivity of higher harmonics has remained relatively unexplored.

In a first step, we examine the differences in the eccentricities between the Glauber and the KLN model, see Figure 5. Here it becomes clear again that while on average differences certainly exist, the width of the distributions is again rather large. This is true both for harmonics present on average as well as event-by-event, such as e_2 , and harmonics only present once fluctuations are taken into account, such as e_3 , suggesting that higher harmonics of jet observables are rather insensitive to initial conditions.

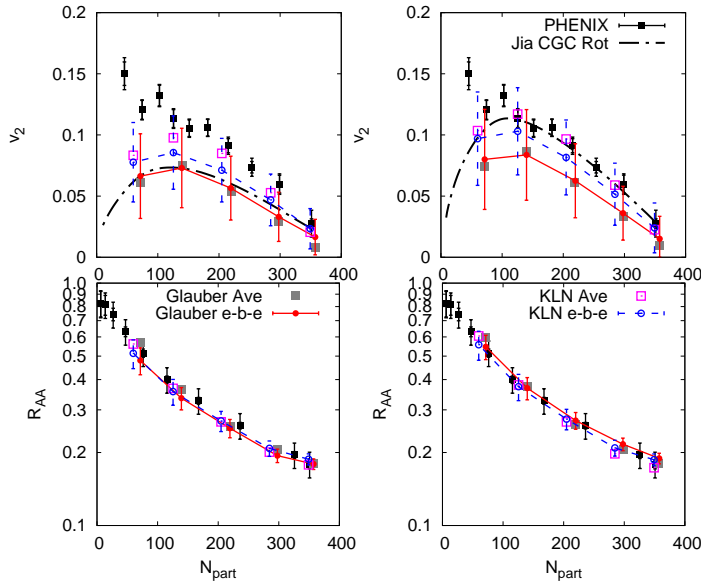


FIG. 3: The fluctuation of v_2 (top panels) and R_{AA} (bottom panels) of high-momentum particles as a function of the number of participants, N_{part} , for $z = 1$ (left panel) and $z = 2$. The data are taken from Ref. [31].

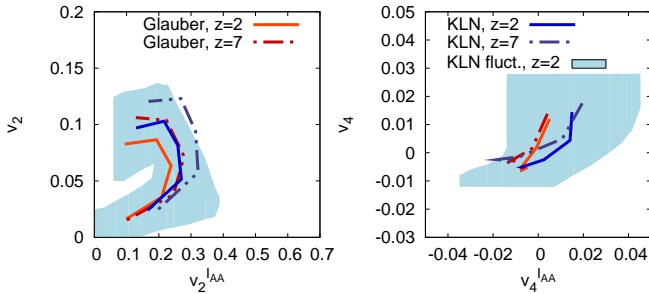


FIG. 4: The fluctuation of the higher Fourier coefficients of dijet observables, v_2^{AA} vs. v_2 (left panel) and v_4^{AA} vs. v_4 (right panel) for the Glauber model (reddish lines) and the KLN model (greyish lines) for $z = 2, 7$. The blue area displays the region covered by the error bars of the KLN scenario for $z = 2$. For the other cases show similar widths.

Fig. 6 displays the mean and the width of $v_3(N_{part})$ and $v_4(N_{part})$ for Glauber and KLN initial conditions. While v_3 is zero unless event-by-event fluctuations are taken into account, v_4 is not too different between average and event-by-event initial conditions. In both cases, however, even a hypothetical ideal experiment capable of determining the impact parameter precisely would be unable to distinguish between Glauber and CGC/KLN initial conditions using only jet harmonics, since event-by-event physical fluctuations are enough to drawn out model sensitivity.

While higher-order coefficients are more sensitive to local gradients, they are also more susceptible to event-by-event fluctuations in initial conditions (hotspots, etc.),

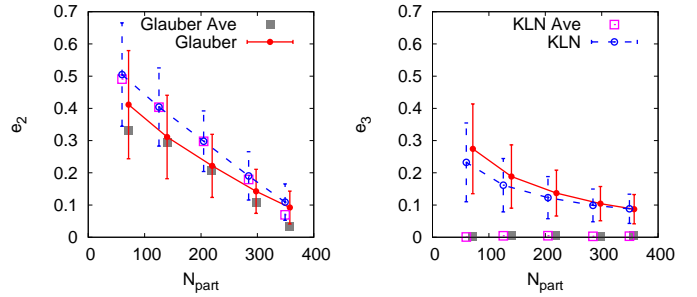


FIG. 5: The eccentricity of the second and third Fourier components of the Glauber and KLN model, both event-by-event (red and blue lines) and averaged (grey and magenta dots). Since e_3 is only present when fluctuations are taken into account, it has to vanish for the averaged analysis.

resulting in a larger $v_{3,4}$ event-by-event fluctuation.

Fig. 7 shows the sensitivity of R_{AA} and v_n to the microscopic mechanism of energy loss, in particular to the power of the path-length dependence z . Here, we consider an impact parameter of $b = 8$ fm that maximizes v_n . As can be seen, once R_{AA} is fixed via the coefficient κ , a residual sensitivity remains mostly in the Fourier components v_2 and v_3 . A clear saturation effect occurs for larger values of z .

Comparing the values of v_2 obtained by the Glauber and the KLN model in Fig. 7 to the data obtained by the PHENIX experiment (black solid and dashed lines representing the datapoint at $N_{part} = 125.7$ and its error bar) [31] show that higher exponents are typically preferred. Note that $z > 2$ is allowed by AdS/CFT [22–25], combined with a significant parton virtuality (which

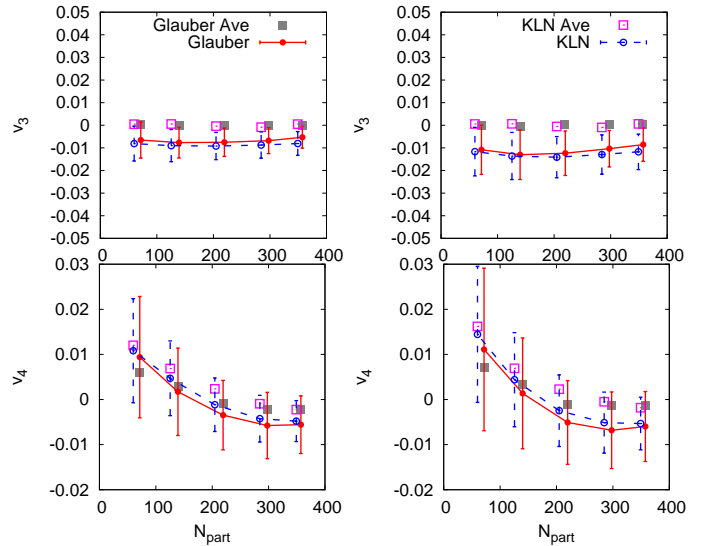


FIG. 6: v_3 (top panels) and v_4 (bottom panels) of high-momentum particles as a function of the number of participants, N_{part} , for $z = 1$ (left panel) and $z = 2$ (right panel).

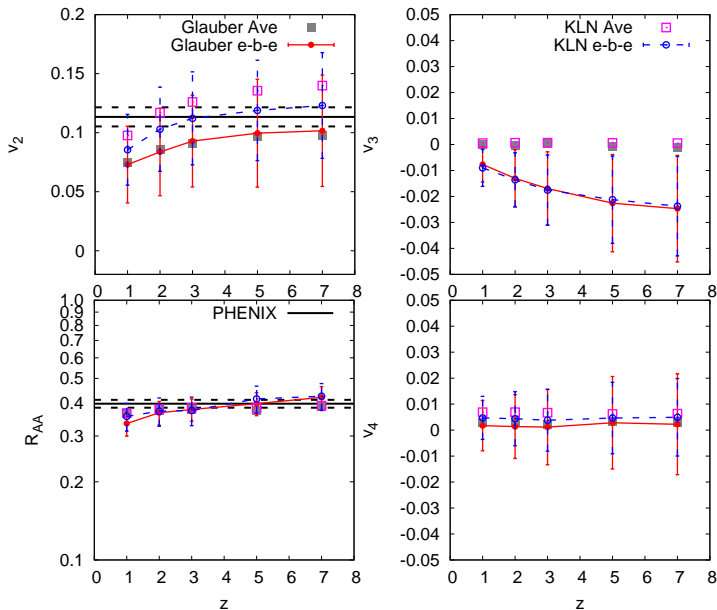


FIG. 7: R_{AA} and v_n of high-momentum particles at an impact parameter of $b = 8$ fm as a function of the path-length exponent z , defined in Eq. (2). pQCD energy loss assumes a $z = 1$ [26, 27, 34], for AdS/CFT on-shell partons $z = 2$, and AdS/CFT off-shell partons are $z > 2$ [22–25]. A clear saturation effect can be seen for all v_n at large z . The data (black solid and dashed lines representing the datapoint at $N_{part} = 125.7$ and its errorbar) are taken from Ref. [31].

is reasonable since the typical stopping length is *not* $l_f \gg 1/T$). In both models the on-shell limit $z = 2$ is disfavored. Since the virtuality can be directly measured in jet-photon collisions, the dependence of the exponent on virtuality could become a quantitative signature of AdS/CFT dynamics. Thus, a simultaneous measurement of v_2 and v_3 could elucidate the microscopic mechanism of jet-energy loss.

However, a question that naturally rises in this context is: Why are v_n 's at high- p_T so insensitive to initial conditions when hydrodynamics shows that the v_n 's of soft particles are extremely sensitive to initial conditions, leading to a systematic error of $\mathcal{O}(100\%)$ in the viscosity

[29]? In fact, the difference between these two regimes is *not* so surprising and can be readily understood physically. While viscous forces are driven by *local gradients* in flow, jet absorption is driven by *global differences* in the integrated $\langle -\kappa P^a \tau^z T^{z-a+2} \rangle$. The two effects are generally not the same and can indeed be very different if the distributions (like initial distributions of energy density in a Lorentz-contracted nucleus) are not smooth.

Both Glauber and KLN initial conditions are tuned to reproduce the observed multiplicity distributions, and hence their $\langle T \rangle$ is similar, even if the *local gradients* of T might be very different. Therefore, it follows that hydrodynamics and tomography lead to very different results.

In conclusion, we investigated higher Fourier harmonics of jet quenching and showed that they are remarkably insensitive to the differences between the Glauber and CGC/KLN model initial conditions. Moreover, we studied the microscopic mechanism of jet-energy loss by including an energy dependence and exploring the exponent z of the jet path-length dependence. We found that while, like in Refs. [26, 27], the $z = 2$ prescription reproduces the measured v_2 well a saturation effect occurs for large z , favoring an energy loss as described by AdS/CFT [22–25]. However, the different $v_n(N_{part})$ vs. $v_n^{IAA}(N_{part})$ correlations between the moments of monojet and dijet nuclear modifications factors remain the most sensitive probe to differentiate between Glauber and CGC/KLN initial conditions.

Acknowledgments

B.B. is supported by the Alexander von Humboldt foundation via a Feodor Lynen fellowship. M.G. and B.B. acknowledge support from DOE under Grant No. DE-FG02-93ER40764. G.T. acknowledges the financial support received from the Helmholtz International Center for FAIR within the framework of the LOEWE program (Landesoffensive zur Entwicklung Wissenschaftlich-Ökonomischer Exzellenz) launched by the State of Hesse. The authors thank A. Dumitru for providing his KLN code to simulate the CGC initial conditions.

[1] M. Gyulassy and L. McLerran, Nucl. Phys. A **750**, 30 (2005); E. V. Shuryak, Nucl. Phys. A **750**, 64 (2005).
[2] I. Arsene *et al.* [BRAHMS Collaboration], Nucl. Phys. A **757**, 1 (2005).
[3] B. B. Back *et al.*, Nucl. Phys. A **757**, 28 (2005).
[4] J. Adams *et al.* [STAR Collaboration], Nucl. Phys. A **757**, 102 (2005).
[5] K. Adcox *et al.* [PHENIX Collaboration], Nucl. Phys. A **757**, 184 (2005).
[6] J. Noronha, M. Gyulassy and G. Torrieri, Phys. Rev. C **82**, 054903 (2010).
[7] M. L. Miller, K. Reygers, S. J. Sanders and P. Steinberg,

Ann. Rev. Nucl. Part. Sci. **57**, 205 (2007).
[8] E. Iancu and R. Venugopalan, arXiv:hep-ph/0303204.
[9] D. Kharzeev and E. Levin, Phys. Lett. B **523**, 79 (2001).
[10] H. J. Drescher, A. Dumitru, C. Gombeaud and J. Y. Ollitrault, Phys. Rev. C **76**, 024905 (2007).
[11] P. Sorensen, J. Phys. G **37**, 094011 (2010).
[12] H. J. Drescher, A. Dumitru, A. Hayashigaki and Y. Nara, Phys. Rev. C **74**, 044905 (2006).
[13] B. Alver, M. Baker, C. Loizides and P. Steinberg, arXiv:0805.4411 [nucl-ex].
[14] R. Andrade, F. Grassi, Y. Hama, T. Kodama and O. J. Socolowski, Phys. Rev. Lett. **97**, 202302 (2006).

- [15] B. Alver and G. Roland, Phys. Rev. C **81**, 054905 (2010).
- [16] M. Gyulassy and X. n. Wang, Nucl. Phys. B **420**, 583 (1994).
- [17] M. Gyulassy, P. Levai and I. Vitev, Phys. Rev. Lett. **85**, 5535 (2000).
- [18] R. Baier, Y. L. Dokshitzer, A. H. Mueller, S. Peigne and D. Schiff, Nucl. Phys. B **484**, 265 (1997).
- [19] U. A. Wiedemann, Nucl. Phys. B **588**, 303 (2000).
- [20] J. w. Qiu and G. F. Sterman, Nucl. Phys. B **353**, 105 (1991).
- [21] P. B. Arnold, G. D. Moore and L. G. Yaffe, JHEP **0111**, 057 (2001).
- [22] S. S. Gubser, D. R. Gulotta, S. S. Pufu and F. D. Rocha, JHEP **0810**, 052 (2008).
- [23] P. M. Chesler, K. Jensen, A. Karch and L. G. Yaffe, Phys. Rev. D **79**, 125015 (2009).
- [24] P. M. Chesler, K. Jensen and A. Karch, Phys. Rev. D **79**, 025021 (2009).
- [25] P. Arnold and D. Vaman, arXiv:1101.2689 [hep-th].
- [26] A. Drees, H. Feng and J. Jia, Phys. Rev. C **71**, 034909 (2005); J. Jia and R. Wei, Phys. Rev. C **82**, 024902 (2010).
- [27] J. Jia, W. A. Horowitz and J. Liao, arXiv:1101.0290 [nucl-th].
- [28] J. D. Bjorken, Phys. Rev. D **27**, 140 (1983).
- [29] H. Song, S. A. Bass, U. W. Heinz, T. Hirano and C. Shen, arXiv:1011.2783 [nucl-th].
- [30] J. Casalderrey-Solana and C. A. Salgado, Acta Phys. Polon. B **38**, 3731 (2007).
- [31] A. Adare *et al.* [PHENIX Collaboration], Phys. Rev. Lett. **105**, 142301 (2010).
- [32] A. Adare *et al.* [PHENIX Collaboration], Phys. Rev. C **78**, 014901 (2008).
- [33] A. Adare *et al.* [The PHENIX Collaboration], Phys. Rev. Lett. **104**, 252301 (2010).
- [34] C. Marquet and T. Renk, Phys. Lett. B **685**, 270 (2010).